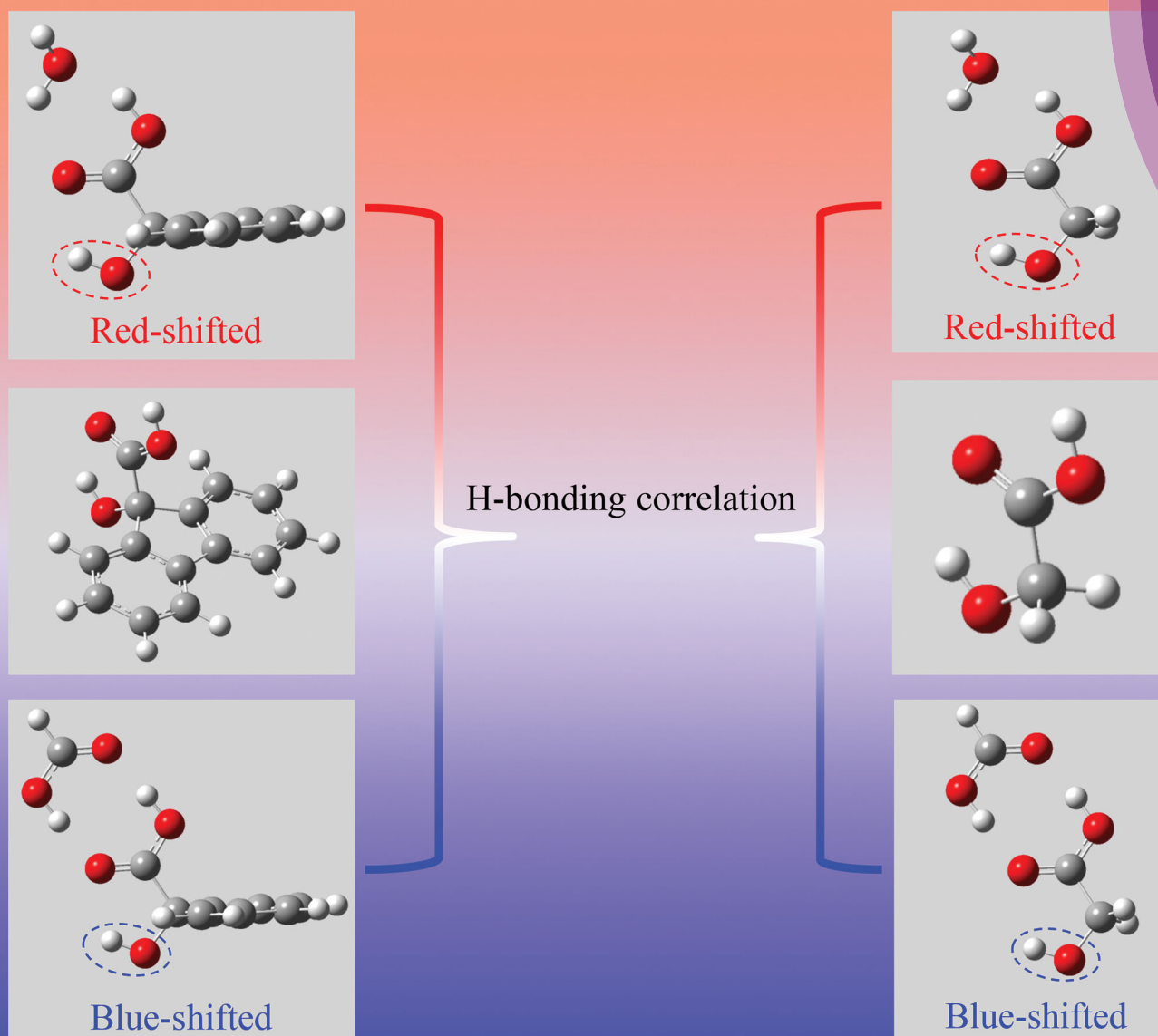
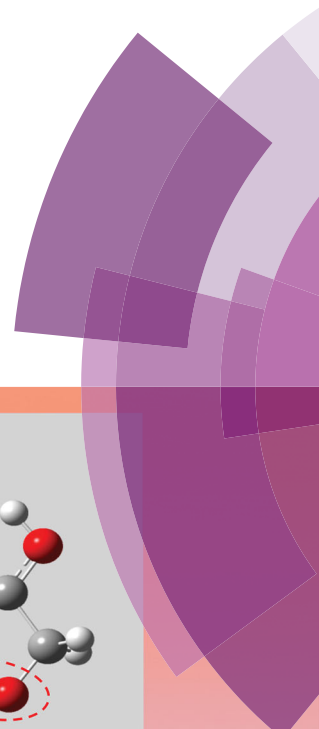


# PCCP

Physical Chemistry Chemical Physics

rsc.li/pccp



ISSN 1463-9076







## PERSPECTIVE

Quanli Gu, Peifeng Su, Yong Xia, Zhijun Yang, Carl O. Trindle and Joseph L. Knee  
Quantitative probing of subtle interactions among H-bonds in alpha hydroxy carboxylic acid complexes



Cite this: *Phys. Chem. Chem. Phys.*,  
2017, **19**, 24399

# Quantitative probing of subtle interactions among H-bonds in alpha hydroxy carboxylic acid complexes

Quanli Gu,  <sup>\*ab</sup> Peifeng Su,  <sup>\*c</sup> Yong Xia, <sup>\*d</sup> Zhijun Yang, <sup>\*a</sup> Carl O. Trindle  <sup>\*e</sup>  
and Joseph L. Knee  <sup>\*f</sup>

Hydrogen (H) bonds are of fundamental importance in a wide range of molecular sciences. While the study of two-center H-bonding A...H is well advanced, much remains to be learned in a quantitative and definitive manner for complexes with multiple H-bonds. Exemplary cases are in the category of alpha hydroxy carboxylic acids, *i.e.*, the complexes of glycolic acid with water and formic acid. In glycolic acid, an intramolecular H-bond forms between the carboxyl group and the alpha OH group. The alpha OH stretching frequency may be affected upon complexing with water or formic acid. Direct study of glycolic acid complexes is unfortunately very difficult. However, an aromatic analogue, 9-hydroxy-9-fluorene carboxylic acid (9HFCA), permits detailed and accurate gas phase spectroscopic studies. Since computational analysis establishes that H-bonding is very similar from glycolic acid complexes to 9HFCA complexes, direct studies on 9HFCA complexes by laser spectroscopy also deduce new and subtle information for glycolic acid complexes in terms of molecular structures, binding strength, and collective effects of multiple H-bonds associated with anti-cooperativity and cooperativity.

Received 12th June 2017,  
Accepted 6th July 2017

DOI: 10.1039/c7cp03917d

rsc.li/pccp

<sup>a</sup> School of Basic Medical Sciences, Xinxiang Medical University, Xinxiang, Henan 453003, China. E-mail: zjyang@xxmu.edu.cn, quanli.gu.phd@gmail.com

<sup>b</sup> Chemistry Department, University of Oklahoma, Norman, Oklahoma 73019, USA

<sup>c</sup> State Key Laboratory of Physical Chemistry of Solid Surfaces, Fujian Provincial Key Laboratory of Theoretical and Computational Chemistry, and College of Chemistry and Chemical Engineering, Xiamen University, Xiamen, Fujian 361005, China. E-mail: supi@xmu.edu.cn

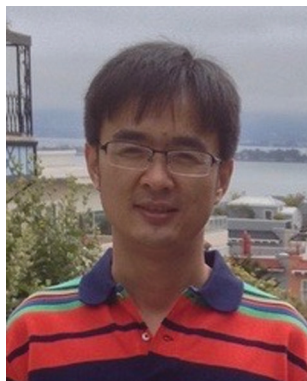
<sup>d</sup> State Key Laboratory of Precision Spectroscopy, School of Physics and Materials Science, East China Normal University, Shanghai 200062, China. E-mail: yxia@phy.ecnu.edu.cn

<sup>e</sup> Chemistry Department, University of Virginia, Charlottesville, Virginia 22904, USA. E-mail: cot@virginia.edu

<sup>f</sup> Chemistry Department, Wesleyan University, Middletown, Connecticut, USA. E-mail: jknee@wesleyan.edu

## Introduction

Hydrogen (H) bonding<sup>1</sup> is of broad interest in molecular sciences, defining liquid water structures and properties,<sup>2</sup> guiding protein dynamics,<sup>3</sup> and assisting proton transfer in ion channels<sup>4</sup> to mention only a few of its significant roles.<sup>5,6</sup> Of course, it has been extensively studied;<sup>7,8</sup> books and review articles on computational and experimental studies are numerous.<sup>9–11</sup> Still, all the subtleties of such interactions are not fully explored.<sup>12</sup> H-Bonding is often associated with shifts in vibrational frequencies.



Quanli Gu

Quanli Gu was born in China, and currently holds two adjoint positions in Xinxiang Medical University and the University of Oklahoma. He has broad interest in experimental and theoretical chemistry. He received his PhD degree in 2009 from Wesleyan University.



Peifeng Su

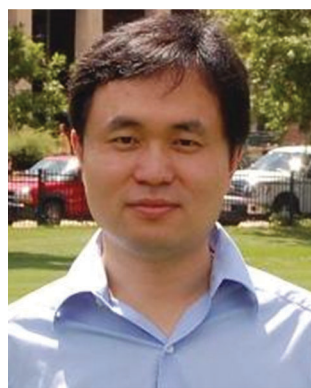
Peifeng Su was born in China, and currently is Associate Professor of Chemistry in Xiamen University. His research focuses on theoretical chemistry. He received his PhD degree in 2007 from Xiamen University.

For example, one normal effect is a red shift in the frequency of the hydroxyl (OH) stretching mode for an OH involved in H-bonding.<sup>13</sup> The red shift can be attributed to a charge transfer from the proton acceptor to the anti-bonding sigma ( $\sigma^*$ ) OH local molecular orbital (LMO) and thus a weakening of the OH bond.<sup>14</sup> The occasional “anomalous blue shift” as in trifluoro-methanol complexes refers to participation by other MOs.<sup>15</sup>

H-Bonding has been extensively characterized for water clusters,<sup>16,17</sup> but also clusters of carboxylic acids.<sup>18–20</sup> One exemplary case is in the category of alpha hydroxy carboxylic acids, *i.e.*, glycolic acid ( $\text{HO}-\text{CH}_2-\text{COOH}$ ), as shown in Fig. 1. In the lowest energy isomer, an intramolecular H-bond forms between the  $\text{C}=\text{O}$  of COOH and the alpha OH. In the glycolic acid–water heterodimer (henceforth it will be called a dimer), water binds to the COOH group of glycolic acid through two distinct intermolecular H-bonds involving its  $\text{C}=\text{O}$  acceptor and OH donor groups. The intramolecular H-bond from the alpha OH may then be affected. As illustrated in Fig. 1a, intuition suggests that relative to its frequency in the glycolic acid monomer, the alpha OH frequency in the water or formic acid clusters would be blue shifted due to the familiar anti-cooperative effect between the intramolecular H-bond and the nearby intermolecular H-bond ( $\text{H} \cdots \text{O}=\text{C}-\text{OH}$ ). We may ask,

will the presence of another intermolecular H-bond ( $\text{O} \cdots \text{HO}-\text{C}=\text{O}$ ) make a difference? If so, will the emerging cooperative effect shift the alpha OH frequency to the red? Which effect, anti-cooperative or cooperative, is dominant among the three H-bonds? Anticipating the ultimate sign of the alpha OH frequency shift starts to be tricky;<sup>21</sup> we are moved to study the subtle interactions of multiple H-bonds in the related systems of alpha hydroxy carboxylic acids and their complexes to see if some interesting patterns of behavior can be discerned.

Glycolic acid is the smallest alpha hydroxy carboxylic acid and has very important applications in wide areas such as astrobiology,<sup>22</sup> organic synthesis, food processing and skin care.<sup>23</sup> However, the study of H-bonding for its complexes with water or formic acid is not an easy task.<sup>24</sup> Glycolic acid has no strong electronic absorption bands, and the ionization potential (IP) lies in the vacuum ultraviolet region,  $\sim 120$  nm; glycolic acid homodimers are also abundant. So, it is quite difficult to synthesize, separate and detect the size-specific heterocomplexes. Not too surprisingly, past work has been unable to unequivocally identify the vibrational frequencies of the two OH groups in glycolic acid – due to the broadening of the IR spectra<sup>24</sup> or the matrix environment complication<sup>25</sup> – not to mention their IR spectra



Yong Xia

*Yong Xia was born in China, and currently is Associate Professor in East China Normal University. His research lies in laser spectroscopy and ultra-cold molecules. He received his PhD degree in 2007 from East China Normal University, and did post-doctoral work in 2010–2011 with Jun Ye at JILA, NIST/CU-boulder.*



Zhijun Yang

*Zhijun Yang was born in China, and currently is Professor in Xinxiang Medical University. His research focuses on analytical spectroscopy and medicinal chemistry. He received his PhD degree in 2005 from Dalian Institute of Chemical Physics.*



Carl O. Trindle

*Carl Trindle was born in USA, and currently is Emeritus Professor in the Chemistry Department, University of Virginia. His work centers on computational modeling and theoretical chemistry. He received his PhD degree in 1967 from Tufts University and was a NSF Postdoctoral Fellow during 1967–1968 at Yale University. After a year as research associate at the Argonne National Laboratory, he joined the faculty at the University of Virginia.*



J. L. Knee

*Joseph Knee was born in USA, and currently is Dean of Natural Sciences and Mathematics and Professor in the Chemistry Department, Wesleyan University. His research areas are ultrafast laser spectroscopy and gas phase molecular dynamics. He received his PhD degree in 1983 from the State University of New York at Stony Brook. He was a Post-doctoral Fellow in 1984–1986 at the California Institute of Technology, after which, he joined the faculty at Wesleyan University.*

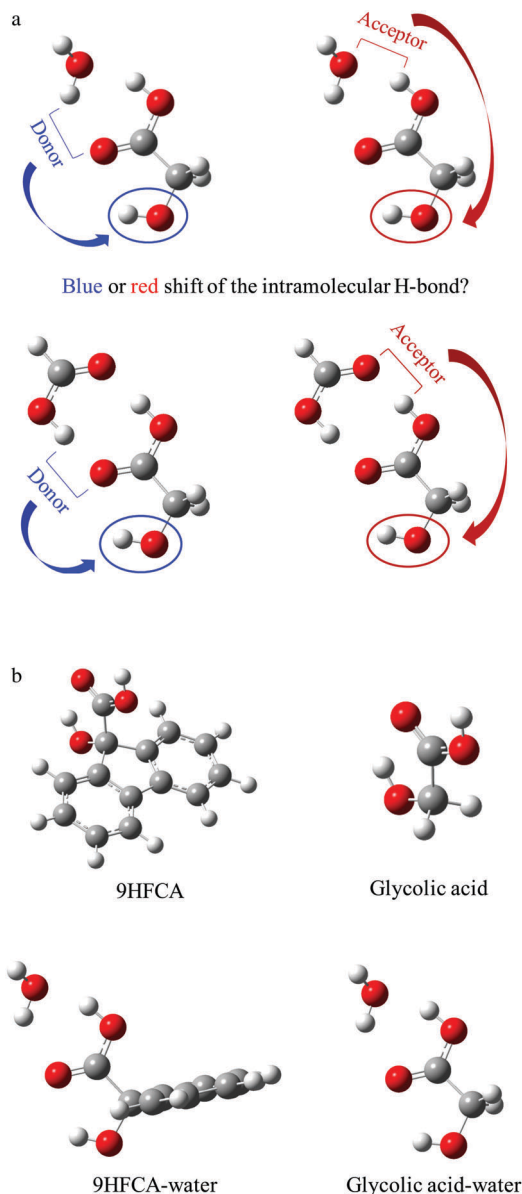


Fig. 1 (a) Glycolic acid and its complexes with water and formic acid. (b) 9HFCA, glycolic acids and their complexes with water.

in the complexes. As well, even seemingly simple questions resist easy answer: In contrast to the water dimer for which the binding energy ( $D_0$ ) is nicely established,<sup>26</sup> the measurement of the binding energy of the glycolic acid–water dimer in fact presents a great challenge to experimentalists. Equally interesting, will water or formic acid affect the alpha OH? How will charge flow, such as in the cation, impact the multiple H-bonding networks in the complexes? What drives the changes? These questions are intriguing and are reviewed here.

In the past 5 years, we have worked diligently to extend H-bonding studies to glycolic acid–water and glycolic acid–formic acid dimers. One principle is that our test systems should be relatively simple so as to be accessible for study both in the laboratory and by theoretical methods. We must seek this information in an analogue of glycolic acid, which contains a

chromophore as well as the central hydroxy acid structure. We have found an aromatic analog, 9-hydroxy-9-fluorene carboxylic acid (9HFCA), in Fig. 1b, to be an excellent choice for H-bonding network studies. 9HFCA contains the chromophore fluorene. The fluorene component has strong ultraviolet (UV) absorption  $\sim 300$  nm, which is well suited to study by electronic and ionization spectroscopy.<sup>27</sup> Upon 9HFCA complexation with water (or formic acid), the remote fluorene moiety appears not to particulate the H-bonding motif. In fact, it will be demonstrated later that the fluorene functional group in 9HFCA does not introduce any complications at all upon glycolic acid moiety complexation with water (or formic acid), so as to offer greater convenience for definitive and quantitative studies by lasers.

In the laboratory, 9HFCA and its complexes were cooled to their vibrational ground states in a supersonic helium beam and then irradiated with tunable high power pulsed lasers, and the IR and UV spectra were recorded using a time of flight mass spectrometer. In this review, in a larger context to other work, five stories are presented and they are connected and involve joint work of experiments and theories. The first demonstrates the excellent analogy between glycolic acid and 9HFCA upon intermolecular H-bonding.<sup>28</sup> The second tells how a most accurate measurement of the  $D_0$  value of 9HFCA–water dimer is obtained,<sup>29</sup> and then with it, the  $D_0$  value of the glycolic acid–water dimer is estimated reliably. The third reveals how the intramolecular H-bond in 9HFCA and glycolic acid can be influenced by a pair of intermolecular H-bonds, interpreting the blue vs. red frequency shifts of the intramolecular H-bond in the complexes.<sup>30</sup> The fourth describes the collective interactions of multiple intra- and intermolecular H-bonds upon ionization of 9HFCA complexes.<sup>31</sup> The fifth quantifies the specific physical interactions contributing to the IP shifts from 9HFCA–water dimer to 9HFCA–formic acid dimer to 9HFCA–hydrofluoric acid dimer, and then non-intuitive physical origins emerge.<sup>32</sup> In the end, we point out further directions for studies of more complex H-bonding networks and related conformational dynamics.

## Experiments

The apparatus to perform the experiments has been documented in previous publications.<sup>33–36</sup> A supersonic helium beam carrying 9HFCA and its complexes was produced by a silicone coated pulsed nozzle (series 9, 20 Hz). For the synthesis of complexes, binding partners were either directly mixed with 9HFCA or seeded in helium *via* a variable flow controller and adjusted so that a significant number of heterodimers were formed with minimal production of larger clusters. Laser spectroscopy was performed downstream in a second chamber at a distance of 10 cm from the nozzle. Tunable IR and UV laser pulses were generated using solid state Nd:YAG lasers pumping tunable dye lasers, followed by non-linear frequency conversions.

The ions or electrons of interest were collected using a standard Wiley–McLaren time-of-flight mass spectrometer.<sup>37</sup> Except for measuring electrons, all spectra were recorded with the mass resolved ion signal. Six types of gas phase spectroscopy



techniques were used to study the H-bonding dynamics. The first is resonance enhanced multiphoton (REMPI) spectroscopy.<sup>38</sup> The REMPI spectra of the first electronically excited state,  $S_1$ , were produced by one-color two-photon ionization processes through  $S_1$  states. The second is UV-UV hole burning spectroscopy, to identify possible isomers.<sup>39</sup> The burning laser frequency was fixed at the electronic origin band, and another UV laser was alternated on vs. off, fired  $\sim 0.1 \mu\text{s}$  later and scanned to obtain the  $S_1$  spectrum. The third and fourth are zero electron kinetic energy (ZEKE),<sup>40</sup> and mass-analyzed threshold ionization (MATI) spectroscopy techniques,<sup>41</sup> to measure the cation spectra *via* a pump-probe double resonance technique. The pump laser was fixed at a particular  $S_1$  vibronic band, and the probe laser was delayed  $\sim 5$  ns and scanned through the very high- $n$  Rydberg states which correspond to the cation structure. The molecules or clusters were excited under field-free conditions. Pulsed electric fields<sup>33</sup> were applied to ionize the high- $n$  Rydberg states and push the resulting electrons or ions toward the detector. The fifth and sixth are IR-UV double resonance<sup>39</sup> and IR-UV action spectroscopy techniques.<sup>42</sup> The IR spectrum was measured *via* an IR-UV double resonance technique. To obtain the IR spectrum, the IR laser was scanned, while the UV laser was introduced 20 ns later and fixed to the  $S_1$  origin transition (monomer or cluster). The IR-UV action spectroscopy experiment was conducted to measure the binding energies in the 9HFCA-water dimer. In this case, the IR laser was fixed on one of the complex bands, and instead the UV laser was scanned to detect any 9HFCA monomer products induced by IR dissociation.

### Calculations

Using basis sets of Pople<sup>43</sup> (6-311++G(d,p)), and Dunning<sup>44</sup> (aug-cc-pVDZ) types, B3LYP,<sup>45</sup> M06-2X<sup>46</sup> and second-order Møller-Plesset<sup>47</sup> (MP2) methods were applied to calculate the isomer with lowest energy, and its associated cluster conformations and energies. Molecular structures, harmonic vibrational frequencies, bond lengths and binding energies were computed in Gaussian 09.<sup>48</sup> Charge analysis was performed by Weinhold's natural bond orbital (NBO) analysis.<sup>49</sup>

To best calculate the  $D_0$  value of the glycolic acid-water dimer, coupled-cluster calculations with complete basis set extrapolation, CCSD(T)/CBS, were performed. To do so, first the glycolic acid-water dimer geometry was optimized on a basis set corrected potential energy surface using MP2/aug-cc-pVTZ, followed by the MP2 single point energy evaluation using a larger basis set, aug-cc-pVQZ. Then, the CCSD(T) single point energy was estimated at these two points to perform the CCSD(T)/CBS extrapolation.<sup>50</sup> Note that the zero point energies (ZPEs) were calculated using MP2/aug-cc-pVTZ. The results are included in Table 1. For the 9HFCA-water dimer, the same type of calculations by CCSD(T)/CBS is prohibitive to us.

To quantify the specific physical interactions contributing to the intermolecular binding strength, the generalized Kohn-Sham energy decomposition analysis (GKS-EDA)<sup>51</sup> was recently developed and performed in the local version of GAMESS.<sup>52</sup> The GKS-EDA scheme performs interaction analysis in the gas phase using various density functionals, including local, hybrid, double

**Table 1**  $D_0$  (in  $\text{cm}^{-1}$ ) calculations for the glycolic acid-water dimer using the basis sets aug-cc-pVTZ and aug-cc-pVQZ, as well as the two-point CBS extrapolation. The ZPE correction was obtained using MP2/aug-cc-pVTZ

	MP2 <sup>a</sup>	MP2 <sup>b</sup>	CCSD(T) <sup>a</sup>	CCSD(T) <sup>b</sup>	CCSD(T)/CBS
$D_0$	2718	2830	2746	2868	2930

<sup>a</sup> aug-cc-pVTZ. <sup>b</sup> aug-cc-pVQZ.

hybrid, range-separated and dispersion corrected functionals, whereas the current version of LMO-EDA<sup>53</sup> cannot work with the range-separated and dispersion corrections. The GKS-EDA also avoids the error of LMO-EDA which arises from the separated treatment of exchange and correlation functionals.

GKS-EDA divides  $D_0$  into electrostatic ( $\Delta E^{\text{ele}}$ ), exchange ( $\Delta E^{\text{ex}}$ ), repulsion ( $\Delta E^{\text{rep}}$ ), polarization ( $\Delta E^{\text{pol}}$ ), correlation ( $\Delta E^{\text{corr}}$ ), dispersion ( $\Delta E^{\text{disp}}$ ) when density functionals have a dispersion correction, as well as geometric relaxation ( $\Delta E(\text{geo})$ ) and harmonic zero point energy ( $\Delta E(\text{ZPE})$ ). The sum of  $\Delta E^{\text{ele}}$ ,  $\Delta E^{\text{ex}}$  and  $\Delta E^{\text{rep}}$  is defined as frozen energy ( $\Delta E^{\text{fro}}$ ).<sup>54</sup>

To maintain consistency,  $D_0$  is the absolute value summing all GKS-EDA terms, namely  $D_0 = |\Delta E^{\text{fro}} + \Delta E^{\text{pol}} + \Delta E^{\text{disp}} + \Delta E^{\text{corr}} + \Delta E(\text{geo}) + \Delta E(\text{ZPE})|$ . Energy terms with a negative sign increase  $D_0$ , while terms with a positive sign decrease  $D_0$ . In the neutral state, in general,  $\Delta E^{\text{rep}}$ ,  $\Delta E(\text{geo})$  and  $\Delta E(\text{ZPE})$  have a positive sign, while the rest terms have a negative sign.

### Five stories

#### H-Bonding analogy between glycolic acid and 9HFCA complexes.

The only difference between 9HFCA and glycolic acid is the fluorene moiety, as seen in Fig. 1. For 9HFCA be a useful substitute for the glycolic acid reference, the fluorene group must not participate in the complex's H-bonding geometry, but 9HFCA must still be able to reflect all effects in the complex's H-bonding network. For glycolic acid and 9HFCA complexes with water, the source of the intermolecular binding strength is presumably the binding motif – the two intermolecular H-bonds formed between the carboxylic acid group and water. So, it is useful to analyze and compare the intermolecular H-bonds in these two dimers.

Several isomers of the 9HFCA-water dimer are possible since water can bind to either the COOH group or the alpha OH group, or even the fluorene moiety. The most stable configuration is water binding to the COOH group through two typical intermolecular H-bonds. Experimentally, only a single conformation of the 9HFCA monomer and its complexes was identified by the UV-UV hole burning experiments, and assigned as the global minimum.<sup>28</sup>

Fig. 2 shows the global minima in the acid-water dimers where water binds to the carboxylic acid group. From glycolic acid-water dimer to 9HFCA-water dimer, by B3LYP/aug-cc-pVDZ calculations quoted below, the harmonic carboxylic OH frequency (no scaling) is similar,  $3318 \text{ cm}^{-1}$  vs.  $3314 \text{ cm}^{-1}$ . The symmetric stretching frequency of water is similar,  $3652 \text{ cm}^{-1}$  vs.  $3659 \text{ cm}^{-1}$ . Two intermolecular H-bond distances are similar,  $1.765 \text{ \AA}$  vs.  $1.765 \text{ \AA}$  and  $2.052 \text{ \AA}$  vs.  $2.062 \text{ \AA}$ , accordingly. This suggests that the intermolecular H-bonds in the glycolic acid-water dimer are minimally distorted by the addition of the fluorene moiety.

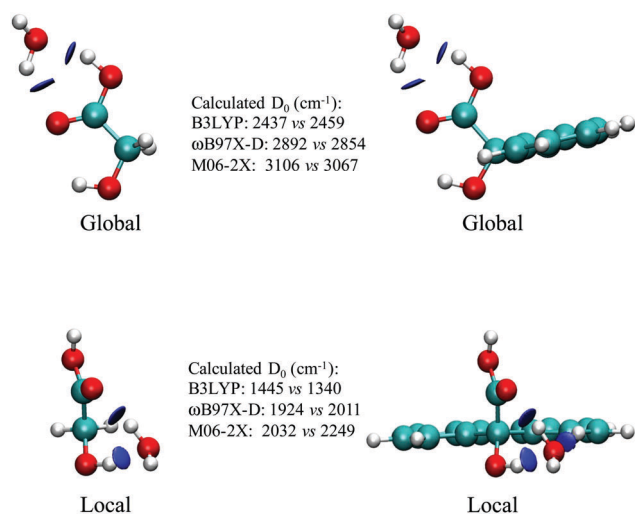


Fig. 2 Calculated structures of glycolic acid–water and 9HFCA–water dimers where water binds to the carboxylic acid group (to form the global minima) and the alcoholic OH group (to form the local minima). The blue color in the NCI plots indicates the intermolecular interactions. The basis set aug-cc-pVDZ was used.

On the other hand, the alpha OH stretching frequency is slightly more different,  $3718\text{ cm}^{-1}$  vs.  $3685\text{ cm}^{-1}$ ; the intramolecular H-bond distance is  $2.111\text{ \AA}$  vs.  $1.996\text{ \AA}$ . Since the intramolecular H-bond in each dimer is not directly participating in the intermolecular interactions, the small difference in the two dimers is expected to be secondary anyway. So, the fluorene moiety (in 9HFCA) may engage a very minor intermolecular interaction as compared to glycolic acid with water. The calculated  $D_0$  numbers are nearly identical,  $2437\text{ cm}^{-1}$  vs.  $2459\text{ cm}^{-1}$  by B3LYP,  $2892\text{ cm}^{-1}$  vs.  $2854\text{ cm}^{-1}$  by  $\omega$ B97X-D, and  $3106\text{ cm}^{-1}$  vs.  $3067\text{ cm}^{-1}$  by M06-2X.

Water can also bind to the alpha OH group in glycolic acid or 9HFCA, as seen in Fig. 2, but this configuration is a high energy local minimum isomer. Interestingly, in this case the fluorene group in 9HFCA starts to engage additional direct H-bonding interaction with water,  $\text{CH}\cdots\text{OH}$ , but absolutely not in a similar glycolic acid–water configuration. So, the analogy between glycolic acid and 9HFCA is compromised in this case. In this configuration, the calculated  $D_0$  values for water complexes with glycolic acid and 9HFCA are much more varying,  $1445\text{ cm}^{-1}$  vs.  $1340\text{ cm}^{-1}$  by B3LYP,  $1924\text{ cm}^{-1}$  vs.  $2011\text{ cm}^{-1}$  by  $\omega$ B97X-D,  $2032\text{ cm}^{-1}$  vs.  $2249\text{ cm}^{-1}$  by M06-2X. In other case where water binds to the  $\pi$  electrons of the fluorene moiety in 9HFCA, the analogy between glycolic acid and 9HFCA in the water complexes is much worse as such a strong interaction ( $\text{OH}-\pi$ ) is completely lacking in the glycolic acid–water dimer.

In addition, the intermolecular interactions for the dimers, in Fig. 2, are visualized in an obvious way by the non-covalent interaction (NCI) plots.<sup>55</sup> From the NCI plots in Fig. 2, for the global minima isomers where water binds to the carboxylic acid group, all signatures of intermolecular H-bonds in the glycolic acid–water dimer, reflected by the blue NCI surfaces, are nearly identical to those in the 9HFCA–water dimer.<sup>28</sup> For the local isomer where water binds to the alpha OH group, however, a

signature of  $\text{CH}\cdots\text{OH}$  intermolecular H-bonding interaction in the 9HFCA–water dimer shows up between the CH group of fluorene and water. So, a stronger influence of the fluorene moiety is evident as water binds to the alpha OH group over the carboxylic acid group. Note that the global minimum isomer of the 9HFCA–water dimer was the only observed one in experiments.

Additional evidence for the analogy between glycolic acid–water and 9HFCA–water dimers (for the global minima) is provided by the GKS-EDA which offers greater details about intermolecular interactions by the identification of specific physical interactions.<sup>51</sup> As seen in Fig. 3, for each term's energies, such as  $\Delta E^{\text{fro}}$ ,  $\Delta E^{\text{pol}}$ ,  $\Delta E^{\text{disp}}$ ,  $\Delta E^{\text{corr}}$ ,  $\Delta E(\text{geo})$ , and  $\Delta E(\text{ZPE})$ , the energy difference between glycolic acid–water and 9HFCA–water dimers, divided by the  $D_0$  of the glycolic acid–water dimer is less than 5% in each method, supporting that the fluorene moiety participates minimal interaction with water. The  $D_0$  difference between 9HFCA–water and glycolic acid–water dimers is even smaller than the individual term's energies. Overall, the GKS-EDA results show that the amount of long-range interaction between water and the fluorene moiety in the 9HFCA–water dimer is minimal.

Furthermore,  $D_0$  calculations of 9HFCA and glycolic acid complexes with a wide range of H-bonding partners,  $\text{NH}_3$ ,  $\text{CH}_3\text{CHO}$ ,  $\text{H}_2\text{NCHO}$ ,  $\text{HCOSH}$ ,  $(\text{H}_2\text{O})_2$ ,  $\text{HCOOH}$ ,  $\text{HCl}$  and  $\text{HF}$ , were performed using M06-2X/aug-cc-pVDZ.<sup>56</sup> The upper panel of Fig. 4 shows the calculated structures for the glycolic acid complexes. As expected, the calculated  $D_0$  value for the glycolic acid complex highly depends on the binding partner. The lower panel of Fig. 4 shows a perfect linear fitting of 9HFCA and glycolic acid complexes over a wide range of the calculated  $D_0$  values, from  $\sim 2000\text{ cm}^{-1}$  to  $\sim 5000\text{ cm}^{-1}$ . The derived  $R^2$  is 0.998 and the slope is 1.039. More calculations using other density functionals and MP2 methods also show the same

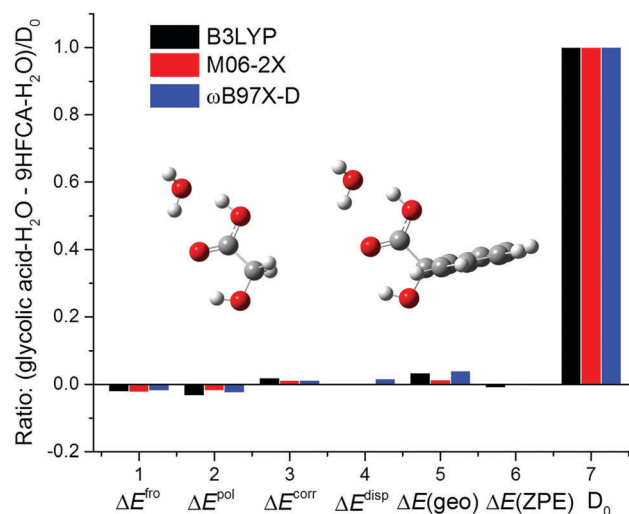


Fig. 3 GKS-EDA of 9HFCA–water and glycolic acid–water dimers. The x-axis lists the GKS-EDA terms and  $D_0$ , and the y-axis corresponds to a ratio, which is the energy difference between glycolic acid–water and 9HFCA–water dimers divided by the  $D_0$  of the glycolic acid–water dimer. Calculations were performed using the basis set aug-cc-pVDZ.

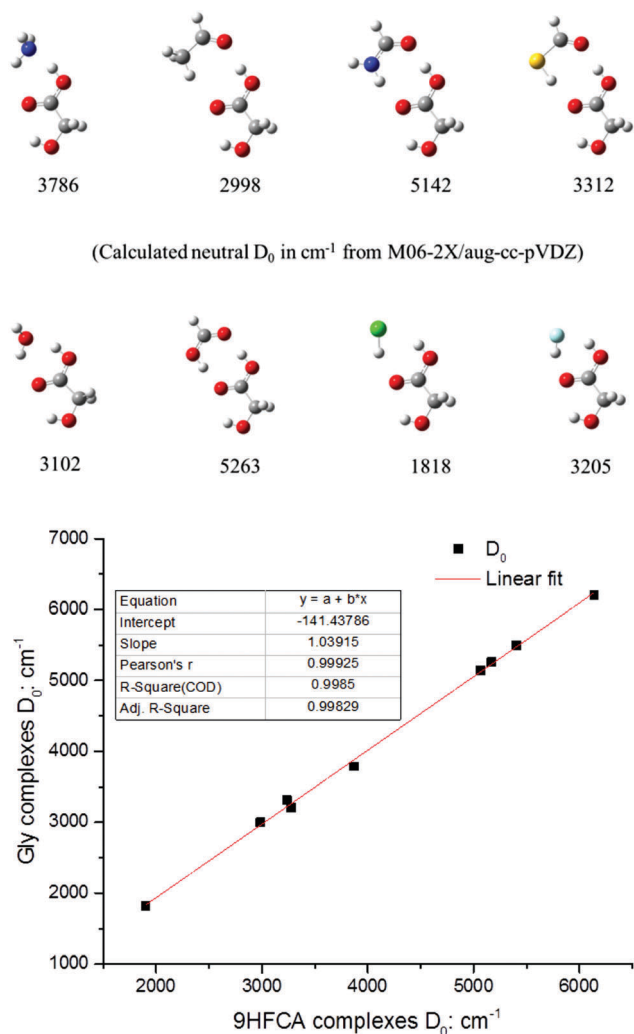


Fig. 4 Upper panel: M06-2X/aug-cc-pVDZ calculated geometries and  $D_0$  values (in  $\text{cm}^{-1}$ ) for glycolic acid complexes. Lower panel: Linear fitting of the  $D_0$  values of 9HFCA and glycolic acid complexes.

linearity. They reinforce the excellent analogy between 9HFCA and glycolic acid upon intermolecular H-bonding.

In short, the fluorene moiety acts as a non-interfering spectator to the intermolecular H-bonding interactions of the glycolic acid–water dimer in that the fluorene group does not participate in the complex's H-bonding geometry, and 9HFCA reflects all effects on the complex's H-bonding network. Therefore, from several aspects, we can determine the plausible properties of glycolic acid complexes with water and formic acid by performing definitive and quantitative experiments on 9HFCA complexes.

**Binding energies of 9HFCA–water and glycolic acid–water dimers.** The glycolic acid–water dimer is a model system, so it is certainly significant to be able to better quantify its binding energy, which will be also useful for kinetic modeling in atmospheric chemistry.<sup>57</sup> There have also been numerous calculations<sup>58–61</sup> of the binding energies of carboxylic acids with water. Extensive computational methods give a wide range of values from 2500 to 3500  $\text{cm}^{-1}$ , and most of this variation is due to the differences between computation methods. More surprisingly, very few

related experimental measurements have been reported on water complexes with any carboxylic acid. Herein, we describe an accurate  $D_0$  measurement for the water–9HFCA dimer,<sup>29</sup> and then with it, infer the  $D_0$  value of the glycolic acid–water dimer.<sup>28</sup>

The IR–UV action spectra with mass detection, in Fig. 5, allow a definitive  $D_0$  measurement for the 9HFCA–water dimer. Pumping the 9HFCA–water dimer's IR absorption band at 3207  $\text{cm}^{-1}$ , three hot bands of the monomer product were observed, while the UV laser was scanned to obtain the REMPI spectrum. The cold monomer origin was not observed in the difference spectrum owing to the large error in the subtraction of the huge background monomer signal. Retuning the IR laser to the nearby 3145  $\text{cm}^{-1}$  band resulted in the observation of only two hot bands. Since the hot band was measured<sup>35</sup> as 67  $\text{cm}^{-1}$ , with these observations, we then confidently bracket the  $D_0$  value as between 2944  $\text{cm}^{-1}$  ( $3145 - 67 \times 3$ ) and 3011  $\text{cm}^{-1}$  ( $3145 - 67 \times 2$ ). The IR excitation at the slightly more energetic band at 3207  $\text{cm}^{-1}$  produced the  $v = 3$  product; this yields a slightly lower upper limit of 3006  $\text{cm}^{-1}$ , providing additional confirmation that the above measurement of the dissociation threshold is correct. So, the  $D_0$  value is determined as  $2975 \pm 30 \text{ cm}^{-1}$ . To our knowledge, this is the most accurate measurement of the binding energy for a carboxylic acid–water dimer.

An additional point is that when the IR laser is fixed at 3145  $\text{cm}^{-1}$ , the energy is above the dissociation threshold and the dissociated products appear within 20 nanoseconds. Dissociation experiments often need to be concerned with the potential metastability of states near the threshold region, mainly because the complex may not dissociate on the short experimental time scale.<sup>62</sup> This is particularly important when determining the lower limit of  $D_0$ . In this case, we are relying on

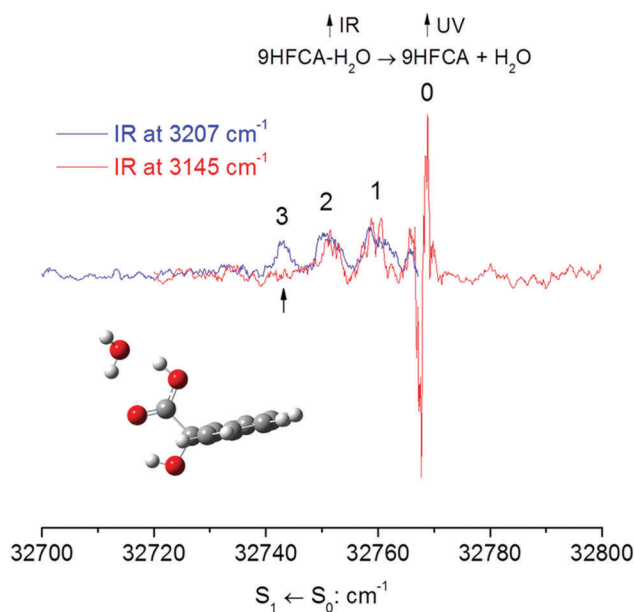


Fig. 5 IR excitation of the 9HFCA–water dimer, followed by UV probe of the 9HFCA monomer product. The plots have been normalized to the  $v = 1$  amplitudes. The arrow points out the missing  $v = 3$  hot band.

product vibrational state distributions to identify the dissociation threshold, thus the time scale is not a concern.

Then, using the fitted slope in Fig. 4 and the experimental  $D_0$  value of the 9HFCA–water dimer, the  $D_0$  value of the glycolic acid–water dimer is estimated to be  $2975 \pm 120 \text{ cm}^{-1}$  ( $2975 \times 0.04$ ), considerably higher than the estimation at the earlier stage,<sup>63</sup>  $2434 \text{ cm}^{-1}$ . Moreover, from the CCSD(T)/CBS method calculations, the  $D_0$  value of the glycolic acid–water dimer is  $2930 \text{ cm}^{-1}$ , very similar to the spectroscopic results of the 9HFCA–water dimer,  $2975 \text{ cm}^{-1}$ , highlighting the necessity and importance of the carefully executed experiment on the 9HFCA–water dimer.

The binding energy of the glycolic acid–water dimer,  $2975 \pm 120 \text{ cm}^{-1}$ , lies in between that of the water dimer,<sup>64</sup>  $1105 \pm 10 \text{ cm}^{-1} \text{ kcal mol}^{-1}$ , and the formic acid dimer,<sup>65</sup>  $4970 \pm 42 \text{ cm}^{-1}$ . Since most of the binding strength in a carboxylic acid–water dimer comes from the two intermolecular H-bonds, our measurement suggests a general binding strength of  $\sim 3000 \text{ cm}^{-1}$  between water and a carboxylic acid, which may be interesting to the wider scientific communities for studying other carboxylic acid–water complexes in atmospheric chemistry<sup>66</sup> and biological medicine.<sup>67</sup> So far, we still have not found another accurate  $D_0$  determination for any other carboxylic acid–water dimer.

**Blue vs. red frequency shifts of the alpha OH.** Since the  $D_0$  value of the glycolic acid–water dimer is determined to be quite large, will water affect the intramolecular H-bond vibrational frequency in glycolic acid? Can the alpha OH in the complex serve as an objective and informative reporter of the complexation? As mentioned before, due to a number of experimental difficulties, there is still no definitive report on the experimental IR spectra of glycolic acid–water and glycolic acid–formic acid dimers. Since the fluorene moiety in 9HFCA does not have any significant impact on the intermolecular H-bonding networks in the complexes, we can measure the IR spectra of 9HFCA complexes<sup>30</sup> and then correlate with those of glycolic acid complexes.<sup>28</sup>

Fig. 6 shows the IR spectra over the range  $3500$  to  $3600 \text{ cm}^{-1}$  of 9HFCA and its complexes with water, formic acid and formamide. 9HFCA clearly displays two separable peaks at  $3538$  and  $3579 \text{ cm}^{-1}$ . The first peak is assigned as the 9-OH stretch, and the second as the carboxylic acid OH stretch. Owing to the intramolecular H-bonding, the 9-OH stretching frequency in 9HFCA is red shifted by more than  $100 \text{ cm}^{-1}$ , relative to the free OH stretch of methanol ( $3684 \text{ cm}^{-1}$ )<sup>68</sup> or phenol ( $3657 \text{ cm}^{-1}$ ).<sup>69</sup> For comparison, the carboxylic OH stretch in 9HFCA is similar to that in the formic acid monomer ( $3570 \text{ cm}^{-1}$ ), which broadens and shifts to  $\sim 3000 \text{ cm}^{-1}$  in the formic acid dimer.<sup>70</sup>

Our study focuses on the further frequency shifts of the 9-OH stretch attending complex formation. The 9-OH stretch frequency is blue shifted by  $13 \text{ cm}^{-1}$  in the formic acid complex, but red shifted by  $11 \text{ cm}^{-1}$  in the formamide complex. For the 9HFCA–water dimer, there are two peaks at  $3531 \text{ cm}^{-1}$  (“red”) and  $3544 \text{ cm}^{-1}$  (“blue”). In the 1:2 9HFCA–(water)<sub>2</sub> complex, the red band remains unchanged and the blue band disappears. 9-OH is not expected to be shifted much by

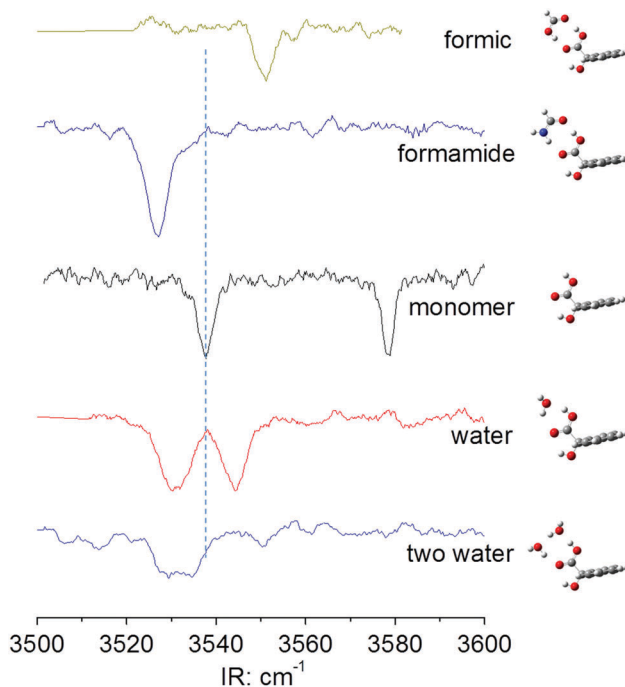


Fig. 6 Experimental IR spectra of the alpha OH stretch frequency in 9HFCA and its complexes. The vertical dash line indicates the alpha OH frequency position in monomer.

addition of one and two water molecules because water preferentially binds to the carboxylic acid group. So, the “red” peak at  $3531 \text{ cm}^{-1}$  is assigned as 9-OH, and the “blue” peak at  $3544 \text{ cm}^{-1}$  as the water symmetric OH stretch. These assignments are also supported by calculations.

Using the MP2 and B3LYP models already defined, we optimized the structures and simulated vibrational spectra of 9HFCA, glycolic acid and their complexes with carboxylic acids, formamide, acetaldehyde, water, thioformic acid, ammonia, hydrochloric acid and hydrofluoric acid.<sup>30</sup> The results of the B3LYP computations and experiments are given in Table 2. The consensus of this array of calculations is that the alpha OH stretch at issue is blue shifted in complexes of 9HFCA (or glycolic acid) with carboxylic acids, hydrochloric acid and hydrofluoric acid, but red shifted in complexes with formamide, ammonia, acetaldehyde, and one or two water molecules.

These computed structures, in Fig. 7a, provide a succinct guide to the source of frequency shifts for the alpha OH in the complexes. Quoted from the B3LYP/6-311++G(d,p) calculations below, the intramolecular H-bond distance is almost unchanged for the entire series of complexes, ranging from  $1.98 \text{ \AA}$  to  $2.00 \text{ \AA}$ . The intermolecular H-bond distance of proton donation from 9HFCA to the binding partner varies over a narrow interval,  $1.64 \text{ \AA}$  to  $1.77 \text{ \AA}$ . In contrast, the intermolecular H-bond distance of proton acceptance from 9HFCA to the partner varies over a much wider range,  $1.70 \text{ \AA}$  to  $2.67 \text{ \AA}$ . 9HFCA’s  $\text{C}=\text{O} \cdots \text{H-X}$  ( $\text{X} = \text{O}, \text{S}, \text{N}$  or  $\text{C}$  from the binding partners) intermolecular H-bond distances correlate with familiar H-bonding strengths, so the salient differences are traced to variation in the partners’ H donation effectiveness. In short, effective H-bonding donation from the



**Table 2** B3LYP/6-311++G(d,p) computed alpha OH frequency shifts ( $\text{cm}^{-1}$ ) in the complexes of 9HFCA and glycolic acid (compared to their monomers)

Complexes	$\text{NH}_3$	$\text{CH}_3\text{CHO}$	$\text{HCONH}_2$	$\text{HCOSH}$	$\text{H}_2\text{O}$	$(\text{H}_2\text{O})_2$	$\text{CH}_3\text{COOH}$	$\text{CH}_3\text{CH}_2\text{COOH}$	$\text{HCOOH}$	$\text{HCl}$	$\text{HF}$
Glycolic acid	−23	−15	−8	−2	−5	−5	1	1	5	11	18
9HFCA	−30	−21	−9	−4	−4	−3	4	4	9	15	25
Experiments <sup>a</sup>	—	—	−11	—	−7	−7	7	7	13	—	—

<sup>a</sup> For 9HFCA complexes.

partner to 9HFCA is associated with blue shifts, while ineffective donation is associated with red shifts. This pattern is perfectly extended to the glycolic acid complexes, as shown in Fig. 7b, pointing out an interesting phenomenon that the alpha OH frequency is red shifted in the glycolic acid–water dimer, and blue shifted in the glycolic acid–formic acid dimer.

Charge transfer also correlates well with the small frequency shifts mentioned above. Plotted in Fig. 7c, regarding the alpha OH group, a longer bond distance or more  $\sigma^*$  electron population relates to red frequency shifts, and *vice versa*. A rationale is readily offered for the blue shifts in frequency. If the partner, such as HF, donates a H atom which engages the  $\text{C}=\text{O}$  of glycolic acid, then the intramolecular H-bonding is weakened. The strength of the intramolecular H-bonding is reduced, so the alpha OH frequency shifts to the blue. It is a familiar case, anti-cooperativity,<sup>14</sup> accompanied by a lesser population in the alcoholic OH  $\sigma^*$  local MO.

How can a (further) red shift in the alpha OH stretch occur? In the limiting  $\text{NH}_3$  case, the partner literally interacts with the  $\text{C}=\text{O}$  of glycolic acid, but H bonds strongly to the carboxylic OH of glycolic acid. The strength of the intramolecular H-bonding is enhanced, so the alpha OH is weakened, accompanied by an additional  $\sigma^*$  population, and a red frequency shift occurs. This shift is a consequence of cooperativity.<sup>71</sup> When the cooperativity is less effective than the anti-cooperativity, as in the formamide and water complexes, the alpha OH is still red shifted, but to a reduced extent compared with the ammonia case. With greater cooperativity, as in the formic acids complex, the alpha OH starts to be blue shifted and most pronounced in the HF case. In short, the blue vs. red frequency shifts of the alpha OH arise from cancellation effects, the consequence of competition between anti-cooperativity and cooperativity associated with the multiple intra- and intermolecular H-bonds in the complexes.

The quantitative correlations among the bond length, frequency shifts and  $\sigma^*$  electron population show that the alpha OH group provides a circumstantial probe of the existence and competing influences of anti-cooperativity and cooperativity among the three H-bonds in the glycolic acid complexes with water and formic acid. Our results and analysis suggest the subtle multiple H-bonding interactions<sup>72</sup> in the glycolic acid–water and glycolic acid–formic acid dimers, which are equally applicable to any other alpha hydroxy carboxylic acids complexes. And they may inspire new experiments to probe quantitatively the H-bonding interactions in variants of these prototypical acid–water and acid–acid complexes, such as beta carboxylic acid complexes.

#### Ionization potentials of 9HFCA H-bonded complexes.

Experimentally, the above vibrational spectroscopy technique has been employed routinely to provide an unambiguous signature

of the intra- and intermolecular H-bonding interactions.<sup>73,74</sup> Unfortunately, in the carboxylic acid dimers, due to the substantial mode couplings arising from the double intermolecular H-bonds, the intermolecular carboxylic OH stretches become messy, structureless, and very broad spanning a wide range from 2600 to 3200  $\text{cm}^{-1}$ .<sup>75</sup> This is also the case for the 9HFCA complex with formic acid, so valuable information may be concealed. Interestingly, by employing two UV lasers, high resolution double resonance photoionization laser spectroscopy avoids this problem. For the first time, we observed the well-defined ionization spectra of 9HFCA, and more interestingly of its complexes with formic acid, acetic acid and benzoic acid.<sup>31</sup> Fig. 8 shows the MATI spectra, plotted as a reference to 9HFCA IP. The lowest energy peak in each spectrum is considered the adiabatic IP, and the higher energy features considered to reflect vibrational excitation. This significant low-frequency progression in the threshold region could have an additional member to the red which may not be observed due to weaker Franck–Condon factors. However, by comparison to the monomer, and given the good signal to noise ratio, particularly for the formic and acetic acid dimers, we expect that all members have been observed. For the benzoic acid cluster, it may not be as definitive but this would not have a major impact on the general conclusions of this work. To compare, the photoionization efficiency (PIE) spectrum of the 9HFCA–water dimer is also included; the superior resolution of the MATI spectra is evident. Note that the sharp rise of the ion signal at the beginning of the PIE spectrum was due to a block of the probe laser. In particular, the IPs for the carboxylic acids are red shifted over a relatively small range, from 545  $\text{cm}^{-1}$  to 1435  $\text{cm}^{-1}$ . For the water complex, it is red shifted by more than 1400  $\text{cm}^{-1}$  from the PIE measurement; its MATI spectrum is not measurable, primarily due to the large geometry change.

The measured IP red shift of 545  $\text{cm}^{-1}$  from monomer to its formic acid dimer is small, compared to other systems such as phenol–water<sup>76</sup> and indole–water clusters<sup>77</sup> in which the IP red shifts are  $\sim 4600$  and  $3200 \text{ cm}^{-1}$ , respectively. For 9HFCA complexes with acetic, formic and benzoic acids, several other isomers are possible for both neutral and cationic states. However, the cyclic structures presented here are the actual global minima, simply because the two parallel intermolecular H-bonds maximize intermolecular interactions in the neutral and cationic states. This has been further confirmed by calculations using extensive density functionals and MP2 methods. Fig. 9a shows the energetics calculated using M06-2X/aug-cc-pVDZ for several geometric isomers in the cationic 9HFCA–formic acid complex. Clearly, the optically accessible isomer with the two parallel intermolecular H-bonds is the actual global minimum.

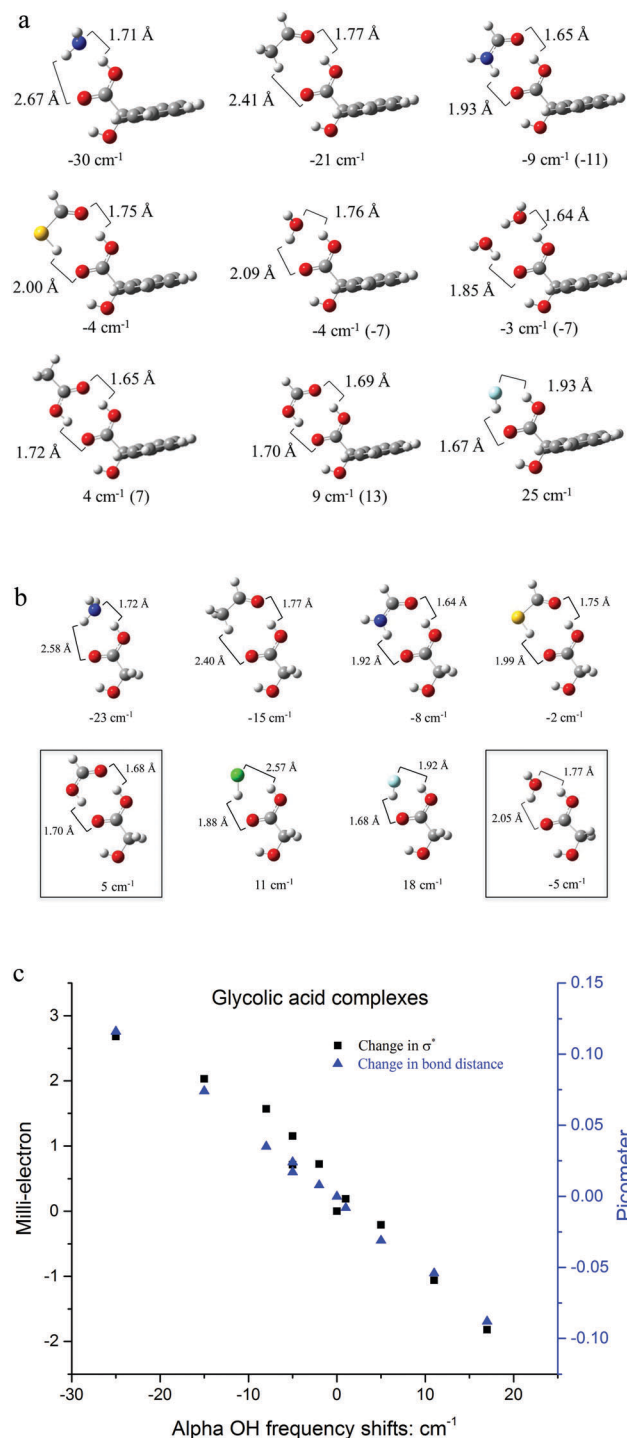


Fig. 7 (a) B3LYP/6-311++G(d,p) computed structures, intermolecular H-bonds distances and alpha OH frequency shifts in 9HFCA complexes. Experimental values appear in brackets. (b) B3LYP/6-311++G(d,p) computed intermolecular H-bonds distances and alpha OH frequency shifts in glycolic acid complexes. (c) B3LYP/6-311++G(d,p) calculated changes in the  $\sigma^*$  and bond distance of the alpha OH in glycolic acid complexes as a function of frequency shifts. They are referenced to the values in the glycolic acid monomer, 967.84 picometers and 14.83 milli-electrons, respectively.

Extensive calculations by B3LYP, M06-2X and MP2 methods show that the  $C_s$  symmetry of the neutral 9HFCA monomer and

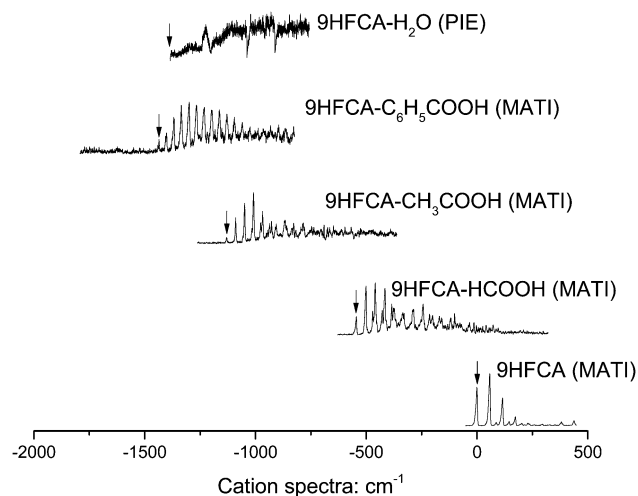


Fig. 8 MATI spectra of 9HFCA and its complexes with formic, acetic and benzoic acids, as well as the PIE spectrum of the 9HFCA–water dimer. The arrows indicate the IP thresholds; the monomer's IP is 64 920 cm<sup>-1</sup>. Note that the sharp rise of the ion signal at the beginning of the PIE spectrum was due to a block of the probe laser.

9HFCA–formic acid complex is retained in the cation. The well-resolved photoionization cation spectrum of 9HFCA is a consequence of the structural stability conferred by the intra-molecular H-bond in all species. The two parallel intermolecular H-bonds in the carboxylic complexes further inhibit drastic geometry changes attending ionization. The vibrational analysis in the cation affirm the locking of the intra- and intermolecular H-bonding networks in the carboxylic complexes. The computed harmonic frequencies for the side chain rocking motion, 58, 43, 38, and 35 cm<sup>-1</sup>, are in excellent agreement with the observed values, 58, 44, 40, and 34 cm<sup>-1</sup> in the monomer and the formic, acetic and benzoic acid complexes, respectively.

To deepen our insight into the IP shifts of 9HFCA H-bonded complexes, the study is extended to a broader range of H-bonding partners from NH<sub>3</sub> to CF<sub>3</sub>COOH. Remarkably, the calculated IP value can be either red or blue shifted in the clusters depending on the H-bonding partner. Fig. 9b shows the calculated structures of the cationic complexes and IP shifts. All the structures, shown in Fig. 9b, are the global minima as verified by extensive density functionals and MP2 calculations. The most extreme red shift is for the NH<sub>3</sub> complex, while the most extreme blue shift is for CF<sub>3</sub>COOH. As the binding partner acts more effectively as a proton donor, as in the sequence of acetaldehyde, formamide to formic acid to trifluoroacetic acid, the shift becomes bluer. This simple geometric criterion and IP shifts lend credence to the hypothesis that the proton donation from 9HFCA is linked to an IP red shift, and the proton donation from the partner is associated with the IP blue shift.

In short, our application of MATI spectroscopy to 9HFCA and its carboxylic acid complexes points to a locking of the multiple intra- and intermolecular H-bonds upon ionization. Shifts in IP of the complexes relative to that of isolated 9HFCA can be ascribed to subtleties of H-bonding: Dominant H donation by 9HFCA tends toward red IP shifts, and strong H donation by the partner tends toward blue IP shifts.

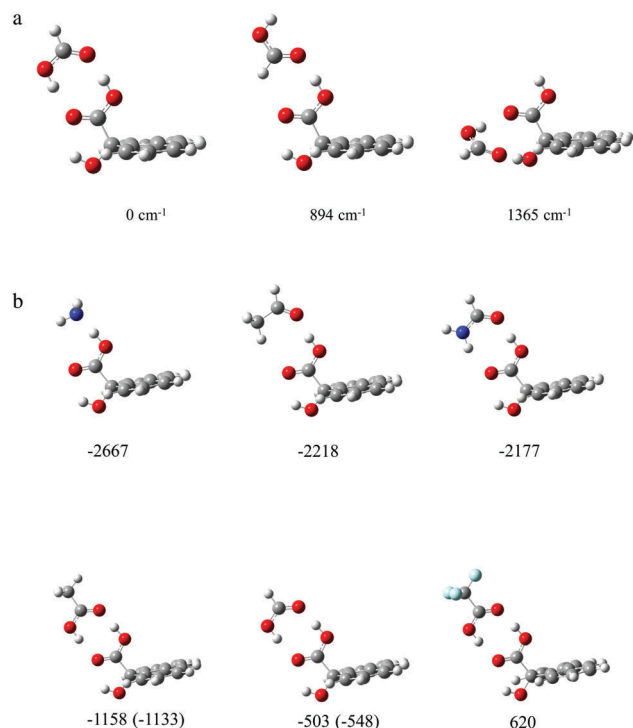


Fig. 9 (a) UM06-2X/aug-cc-pVDZ calculated conformational energetics (in  $\text{cm}^{-1}$ ) for the cationic 9HFCA-formic acid dimer. (b) B3LYP/6-311++G(d,p) calculated cation structures and IP shifts (in  $\text{cm}^{-1}$ ) for 9HFCA H-bonded complexes (relative to 9HFCA). Experimental numbers appear in brackets.

**Physical origins of IP shifts of 9HFCA complexes with water, formic acid and hydrofluoric acid.** We have established the value of IP shifts in diagnosing the details of H-bonding in 9HFCA complexes with a variety of H-bonding species. But how can we think about the causes of the IP shifts? What drives the IP shifts – from 9HFCA-water dimer to 9HFCA-formic acid dimer to 9HFCA-HF dimer – is elusive.

From a structural point of view, in Fig. 10a, based on B3LYP/6-311++G(d,p) calculations (confirmed by M06-2X and MP2), ionization in 9HFCA and its H-bonded complexes has the slight effect of weakening the intramolecular H-bonding (the H-bond distance barely changes). Ionization has a more dramatic impact on the geometry of the intermolecular H-bonds. In each case, the ionization strengthens the intermolecular H-bond in which 9HFCA is the H donor, and weakens the intermolecular H-bond in which 9HFCA is the H acceptor; this is due to the charge flow from the fluorene moiety to the glycolic acid component.

To reveal the non-intuitive physical origins, GKS-EDA is particularly a useful approach, which also provides a quantitative understanding of specific physical interactions.<sup>51</sup> The IP shifts from monomer to complex are equal to the differences of  $D_0$  between neutral and cationic complexes,<sup>32</sup> so we focus on their differences in each of these GKS-EDA terms. They were computed by B3LYP, M06-2X, and  $\omega$ B97X-D methods using a 6-311++G(d,p) basis set, and plotted in Fig. 10b. In the estimation of the energy differences (cationic-neutral) for each term, all three methods are consistent. The calculated IP shifts also agree with the

experimental measurements, more than  $1400 \text{ cm}^{-1}$  to the red for the 9HFCA-water dimer and  $545 \text{ cm}^{-1}$  to the red for the 9HFCA-formic acid dimer.

From neutral to cationic complexes, the changes of  $\Delta E^{\text{fro}}$  and  $\Delta E^{\text{pol}}$  contribute most significantly to the IP shifts, and are related to the changes in the H-bonding network. The changes of rest terms are minor, and so will not be discussed here.

For the 9HFCA-water dimer, upon ionization, the breakup of the H-bonding network to the single H-bond results in a decrease of the frozen electron density interaction  $\Delta E^{\text{fro}}$ . Moreover, the newly strengthened intermolecular H-bond in the cation has a much higher polarization energy, consistent with its shorter intermolecular H-bond distance and a red shifted carboxylic OH frequency. The changes of  $\Delta E^{\text{fro}}$  and  $\Delta E^{\text{pol}}$  are toward the same direction – negative, to constitute the greater part of the red IP shifts.

For the 9HFCA-formic acid dimer, upon ionization, the H-bonding network is preserved, thanks to the competitive parallel H-bond donation from formic acid. Consequently, the change of  $\Delta E^{\text{fro}}$  is surprisingly positive – this is starkly different

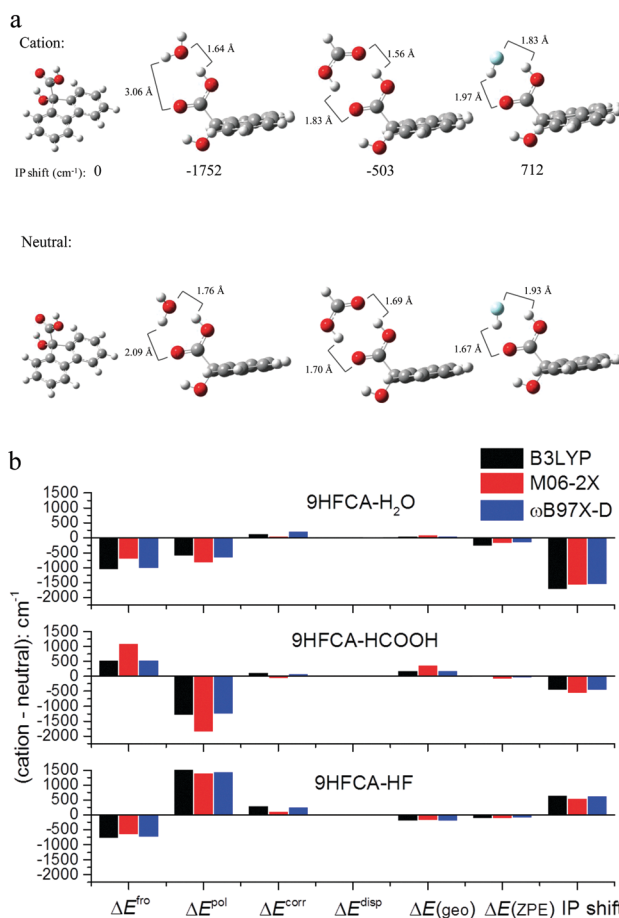


Fig. 10 (a) B3LYP/6-311++G(d,p) calculated geometries and IP shifts ( $\text{cm}^{-1}$ ) for 9HFCA and its complexes with water, formic acid and hydrofluoric acid. (b) GKS-EDA results for 9HFCA complexes with water, formic acid and hydrofluoric acid. The x-axis lists the GKS-EDA terms and IP shift, and the y-axis is the energy difference between cationic and neutral complexes (in  $\text{cm}^{-1}$ ). All values were computed using the basis set 6-311++G(d,p).

from the 9HFCA–water dimer – shifting the IP toward blue. The change of  $\Delta E^{\text{pol}}$ , on the other hand, is the biggest factor, and still negative, shifting the IP toward red. The partial cancellation then results in an IP still shifted to the red, but by a much smaller amount than seen for the 9HFCA–water dimer.

For the 9HFCA–hydrofluoric acid dimer, upon ionization, the H-bonding network is not broken, but the angles of the two intermolecular H-bonds change alongside the bond lengths. Consequently, the change of  $\Delta E^{\text{fro}}$  is negative, shifting the IP to the red. The change of  $\Delta E^{\text{pol}}$ , however, is the largest factor and positive – this is different from the 9HFCA–water and 9HFCA–formic acid dimers – shifting the IP toward blue. So, the partial cancellation results in an IP shifted to the blue.

One more interesting point is for dispersion related interactions,<sup>78</sup>  $\Delta E^{\text{corr}} + \Delta E^{\text{disp}}$ . Upon ionization, the accompanying change of  $\Delta E^{\text{corr}}$  or  $\Delta E^{\text{disp}}$  is very small among the three complexes. This indicates that the dispersion related energies are not sensitive to the dramatic changes in the H-bonding network and charge flow. As such, the B3LYP method employed can also reproduce the IP shifts even if this functional has notoriously poor dispersion/correlation treatments.

In short, the explanatory power of the GKS-EDA energetic components coupled with the computed geometric changes leads to non-intuitive insights into the intermolecular interactions from neutral to cationic complexes, such as repulsion from frozen interaction and attraction from polarization interaction which are related to the H-bonding networks of 9HFCA complexes such as with water, formic acid and hydrofluoric acid.

## Concluding remarks

Complementing previous reviews, the quantitative and definitive studies highlight subtle interactions among H-bonds in alpha hydroxy carboxylic acid complexes. The significance of this review lies in five stories: (1) we demonstrate the excellent analogy between 9HFCA and glycolic acid upon intermolecular H-bonding with a number of partners such as water and formic acid. (2) We obtain the accurate  $D_0$  value for the 9HFCA–water dimer, and extend this value to evaluate the binding energy for the glycolic acid–water dimer with a much better accuracy than previous reports. (3) Our infrared spectra of 9HFCA complexes are new and interesting in the way in which the alpha OH group is used as a sensitive reporter of the existence and competing influences of anti-cooperative and cooperative activities, which are extendable to the glycolic acid complexes. (4) In our 9HFCA–formic acid dimer, we observe that the complicated H-bonding network remains intact upon ionization, and ionization potentials can be red or blue shifted due to the competition of the two intermolecular H-bonds. (5) Our computational work supports the experiments, and the GKS-EDA provides non-intuitive physical insights and quantitative understanding of blue vs. red IP shifts. Overall, these new outcomes can be easily adapted to describe other alpha or beta hydroxy carboxylic acid systems. Looking forward to the future, this review will invoke further studies, as shown in Fig. 11, for conformational dynamics, vibrational

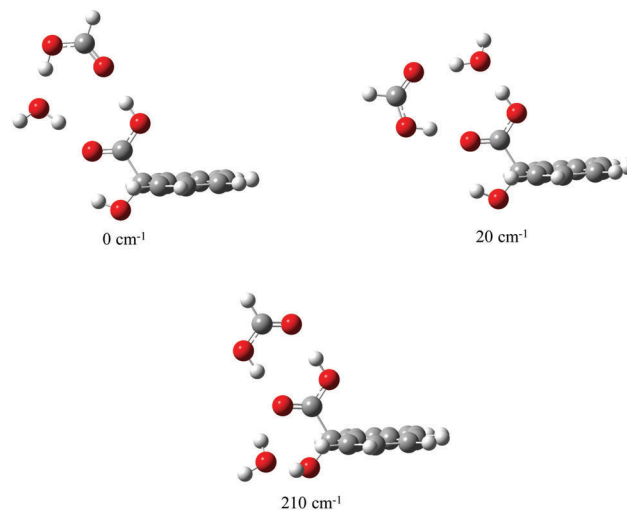


Fig. 11 M06-2X/6-311++G(d,p) calculated energetics (in  $\text{cm}^{-1}$ ) for the neutral complex of 9HFCA–water–formic acid.

de-coupling of intermolecular modes and charge transfer pathways alongside the H-bonding networks while increasing the molecular complexity *via* mixing two and even three carboxylic acids with water.

## Acknowledgements

Q. G. thanks the Barbara A. Body Foundation fellowship. P. S. acknowledges the grants from the Natural Science Foundation of China (No. 21373165 and 21573176), and the Fundamental Research Funds for the Central Universities, China (No. 20720150037). Y. X. acknowledges the grant from the National Natural Science Foundation of China (No. 11374100).

## References

- 1 E. Arunan, G. R. Desiraju, R. A. Klein, J. Sadlej, S. Scheiner, I. Alkorta, D. C. Clary, R. H. Crabtree, J. J. Dannenberg, P. Hobza, H. G. Kjaergaard, A. C. Legon, B. Mennucci and D. J. Nesbitt, *Pure Appl. Chem.*, 2011, **83**, 1619–1636.
- 2 A. Henao, S. Busch, E. Guardia, J. L. Tamarit and L. C. Pardo, *Phys. Chem. Chem. Phys.*, 2016, **18**, 19420–19425.
- 3 P. K. Verma, H. Lee, J. Y. Park, J. H. Lim, M. Maj, J. H. Choi, K. W. Kwak and M. Cho, *J. Phys. Chem. Lett.*, 2015, **6**, 2773–2779.
- 4 Y. Nishihara and A. Kitao, *Proc. Natl. Acad. Sci. U. S. A.*, 2015, **112**, 7737–7742.
- 5 O. F. Mohammed, O. H. Kwon, C. M. Othon and A. H. Zewail, *Angew. Chem., Int. Ed.*, 2009, **48**, 6251–6256.
- 6 E. H. Krenske, A. Patel and K. N. Houk, *J. Am. Chem. Soc.*, 2013, **135**, 17638–17642.
- 7 E. V. Beletskiy, J. Schmidt, X. B. Wang and S. R. Kass, *J. Am. Chem. Soc.*, 2012, **134**, 18534–18537.
- 8 A. Shokri, Y. Wang, G. A. O'Doherty, X. B. Wang and S. R. Kass, *J. Am. Chem. Soc.*, 2013, **135**, 17919–17924.



- 9 S. Scheiner, *Hydrogen Bonding: A Theoretical Perspective*, Oxford University Press, New York, 1997, pp. 1–375.
- 10 P. Hobza and J. Řezáč, Noncovalent interactions, a special issue of, *Chem. Rev.*, 2016, **116**, 4911–5687; Especially A. K. Samanta, Y. Wang, J. S. Mancini, J. M. Bowman and H. Reisler, *Chem. Rev.*, 2016, **116**, 4913–4936; O. Dopfer and M. Fujii, *Chem. Rev.*, 2016, **116**, 5432–5463.
- 11 A. S. Mahadevi and G. N. Sastry, *Chem. Rev.*, 2016, **116**, 2775–2825.
- 12 J. O. Richardson, C. Perez, S. Lobsiger, A. A. Reid, B. Temelso, G. C. Shields, Z. Kisiel, D. J. Wales, B. H. Pate and S. C. Althorpe, *Science*, 2016, **351**, 1310–1313.
- 13 M. Rozenberg, A. Loewenschuss and Y. Marcus, *Phys. Chem. Chem. Phys.*, 2000, **2**, 2699–2702.
- 14 F. Weinhold and R. A. Klein, *Mol. Phys.*, 2012, **110**, 565–579.
- 15 X. Li, L. Liu and H. B. Schlegel, *J. Am. Chem. Soc.*, 2002, **124**, 9639–9647.
- 16 C. Perez, M. T. Muckle, D. P. Zaleski, N. A. Seifert, B. Temelso, G. C. Shields, Z. Kisiel and B. H. Pate, *Science*, 2012, **336**, 897–901.
- 17 J. Howard and G. Tschumper, *J. Chem. Theory Comput.*, 2015, **11**, 2126–2136.
- 18 Y. Chang, Y. Yamaguchi, W. Miller and H. Schaefer III, *J. Am. Chem. Soc.*, 1987, **109**, 7245–7253.
- 19 A. Slater, L. Perdigo, P. Beton and N. Champness, *Acc. Chem. Res.*, 2014, **47**, 3417–3427.
- 20 O. Birer and M. Havenith, *Annu. Rev. Phys. Chem.*, 2009, **60**, 263–275.
- 21 A. J. Thakkar, N. E. Kassimi and S. W. Hu, *Chem. Phys. Lett.*, 2004, **387**, 142–148.
- 22 M. Nuevo, J. H. Bredehoft, U. J. Meierhenrich, L. d'Hendecourt and W. H. P. Thiemann, *Astrobiology*, 2010, **10**, 245.
- 23 US Food and Drug Administration (FDA) website, [www.fda.gov](http://www.fda.gov).
- 24 D. K. Havey, K. J. Feierabend and V. Vaida, *J. Phys. Chem. A*, 2004, **108**, 9069–9073.
- 25 A. Halasa, L. Lapinski, I. Reva, H. Rostkowska, R. Fausto and M. J. Nowak, *J. Phys. Chem. A*, 2014, **118**, 5626–5635.
- 26 B. E. Rocher-Casterline, L. C. Ch'ng, A. K. Mollner and H. Reisler, *J. Chem. Phys.*, 2011, **134**, 211101.
- 27 J. M. Smith, C. Lakshminarayan and J. L. Knee, *J. Chem. Phys.*, 1990, **93**, 4475–4476.
- 28 Q. Gu, D. Shen, Z. Tang, W. Wu, P. Su, Y. Xia, Z. Yang and C. O. Trindle, *Phys. Chem. Chem. Phys.*, 2017, **19**, 14238–14247.
- 29 Q. Gu and J. L. Knee, *J. Chem. Phys.*, 2012, **136**, 171101.
- 30 Q. Gu, C. Trindle and J. L. Knee, *J. Chem. Phys.*, 2012, **137**, 091101.
- 31 Z. Yang, Q. Gu, C. O. Trindle and J. L. Knee, *J. Chem. Phys.*, 2013, **139**, 151101.
- 32 Q. Gu, Z. Tang, P. Su, W. Wu, Z. Yang, C. Trindle and J. L. Knee, *J. Chem. Phys.*, 2016, **145**, 051101.
- 33 Q. Gu and J. L. Knee, *J. Chem. Phys.*, 2008, **128**, 064311.
- 34 Q. Gu and J. L. Knee, *J. Chem. Phys.*, 2012, **137**, 104312.
- 35 Q. Gu, C. Trindle and J. L. Knee, *J. Phys. Chem. A*, 2014, **118**, 4982–4987.
- 36 Z. Yang, Q. Gu, C. Trindle and J. L. Knee, *J. Chem. Phys.*, 2015, **143**, 034308.
- 37 W. C. Wiley and I. H. McLaren, *Rev. Sci. Instrum.*, 1955, **26**, 1150–1157.
- 38 P. M. Johnson, *Acc. Chem. Res.*, 1980, **13**, 20–26.
- 39 T. S. Zwier, *J. Phys. Chem. A*, 2006, **110**, 4133–4150.
- 40 C. E. Dessent and K. Muller-Dethlefs, *Chem. Rev.*, 2000, **100**, 3999–4022.
- 41 L. C. Zhu and P. Johnson, *J. Chem. Phys.*, 1991, **94**, 5769.
- 42 B. A. O'Donnell, E. X. Li, M. I. Lester and J. S. Francisco, *Proc. Natl. Acad. Sci. U. S. A.*, 2008, **105**, 12678–12683.
- 43 R. Ditchfield, W. J. Hehre and J. A. Pople, *J. Chem. Phys.*, 1971, **54**, 724–728.
- 44 T. H. Dunning, *J. Chem. Phys.*, 1989, **90**, 1007–1023.
- 45 A. D. Becke, *J. Chem. Phys.*, 2014, **140**, 18A301.
- 46 Y. Zhao and D. G. Truhlar, *Acc. Chem. Res.*, 2008, **41**, 157–167.
- 47 M. J. Frisch, M. Head-Gordon and J. A. Pople, *Chem. Phys. Lett.*, 1980, **166**, 275–280.
- 48 M. J. Frisch, *et al.*, *Gaussian 09, Revision D.01*, Gaussian, Inc., Wallingford CT, 2009.
- 49 A. E. Reed, R. B. Weinstock and F. Weinhold, *J. Chem. Phys.*, 1985, **83**, 735–746.
- 50 T. Helgaker, W. Klopper, H. Koch and J. Noga, *J. Chem. Phys.*, 1997, **106**, 9639.
- 51 P. Su, Z. Jiang, Z. Chen and W. Wu, *J. Phys. Chem. A*, 2014, **118**, 2531–2542.
- 52 M. W. Schmidt, K. K. Baldridge, J. A. Boatz, S. T. Elbert, M. S. Gordon, J. H. Jensen, S. Koseki, N. Matsunaga, K. A. Nguyen, S. J. Su, T. L. Windus, M. Dupuis and J. A. Montgomery, *J. Comput. Chem.*, 1993, **14**, 1347–1363.
- 53 P. Su and H. Li, *J. Chem. Phys.*, 2009, **131**, 014102.
- 54 P. R. Horn and M. A. Head-Gordon, *J. Chem. Phys.*, 2016, **144**, 084118.
- 55 J. Contreras-Garcia, E. R. Johnson, S. Keinan, R. Chaudret, J. P. Piquemal, D. N. Beratan and W. Yang, *J. Chem. Theory Comput.*, 2011, **7**, 625–632.
- 56 L. A. Burns, A. Vazquez-Mayagoitia, B. G. Sumpter and C. D. Sherrill, *J. Chem. Phys.*, 2011, **134**, 084107.
- 57 S. D. Le Picard, M. Tizniti, A. Canosa, I. R. Sims and I. W. Smith, *Science*, 2010, **328**, 1258–1262.
- 58 S. Aloisio, P. E. Hintze and V. Vaida, *J. Phys. Chem. A*, 2002, **106**, 363–370.
- 59 Q. Gao and K. T. Leung, *J. Chem. Phys.*, 2005, **123**, 074325.
- 60 A. K. Tiwari and N. Sathyamurthy, *J. Phys. Chem. A*, 2006, **110**, 5960–5964.
- 61 E. G. Schnitzler and W. Jager, *Phys. Chem. Chem. Phys.*, 2014, **16**, 2305–2314.
- 62 J. R. Clarkson, J. M. Herbert and T. S. Zwier, *J. Chem. Phys.*, 2007, **126**, 134306.
- 63 D. K. Havey, K. J. Feierabend, K. Takahashi, R. T. Skodje and V. Vaida, *J. Phys. Chem. A*, 2006, **110**, 6439–6446.
- 64 B. E. Rocher-Casterline, L. C. Ch'ng, A. K. Mollner and H. Reisler, *J. Chem. Phys.*, 2011, **134**, 211101.
- 65 F. Kollipost, R. W. Larsen, A. V. Domanskaya, M. Norenberg and M. A. Suhm, *J. Chem. Phys.*, 2012, **136**, 151101.
- 66 V. Vaida, *J. Chem. Phys.*, 2011, **135**, 020901.

- 67 A. J. Smith, X. Zhang, A. G. Leach and K. N. Houk, *J. Med. Chem.*, 2009, **52**, 225–233.
- 68 Y. J. Hu and E. R. Bernstein, *J. Chem. Phys.*, 2006, **125**, 154306.
- 69 T. Watanabe, T. Ebata, S. Tanabe and N. Mikami, *J. Chem. Phys.*, 1996, **105**, 408–419.
- 70 C. Trindle and Y. J. Ilhan, *J. Chem. Theory Comput.*, 2008, **4**, 533–541.
- 71 V. L. Deringer, U. Englert and R. Dronskowski, *Biomacromolecules*, 2016, **17**, 996–1003.
- 72 J. M. Guevara-Vela, E. Romero-Montalvo, V. A. M. Gómez, R. Chávez-Calvillo, M. García-Revilla, E. Francisco, Á. M. Pendás and T. Rocha-Rinza, *Phys. Chem. Chem. Phys.*, 2016, **18**, 19557–19566.
- 73 K. Tanabe, M. Miyazaki, M. Schmies, A. Patzer, M. Schutz, H. Sekiya, M. Sakai, O. Dopfer and M. Fujii, *Angew. Chem., Int. Ed.*, 2012, **51**, 6604–6607.
- 74 N. S. Nagornova, T. R. Rizzo and O. V. Boyarkin, *Science*, 2012, **336**, 320–323.
- 75 G. M. Florio, T. S. Zwier, E. M. Myshakin, J. D. Jordan and E. L. Sibert, *J. Chem. Phys.*, 2003, **118**, 1735–1746.
- 76 J. E. Braun and H. J. Neusser, *Mass Spectrom. Rev.*, 2002, **21**, 16–36.
- 77 J. E. Braun, T. L. Grebner and H. J. Neusser, *J. Phys. Chem. A*, 1998, **102**, 3273–3278.
- 78 S. Grimme, A. Hansen, J. G. Brandenburg and C. Bannwarth, *Chem. Rev.*, 2016, **116**, 5105–5154.